Photoreaction of Thioxanthone with Indolic and Phenolic Derivatives of Biological Relevance: Magnetic Field Effect Study

Doyel Das and Deb Narayan Nath*

Department of Physical Chemistry Indian Association for the Cultivation of Science, Jadavpur, Kolkata 700 032, India

Received: August 1, 2008; Revised Manuscript Received: October 1, 2008

The photoinduced reaction of thioxanthone (TX) with various indolic and phenolic derivatives and amino acids like tryptophan and tyrosine has been monitored in sodium dodecyl sulfate micellar medium. Laser flash photolysis and magnetic field effect (MFE) experiments have been used to study the dynamics of the radical pairs. The quenching rate constant with different quenchers in SDS micellar solution has been measured. For indoles the electron-transfer reaction has been found to be followed by proton transfer from the donor molecule, which gives rise to the TX ketyl radical. On the other hand, the electron-transfer reaction in the case of phenols is preceded with formation of a hydrogen-bonded exciplex. The extent of the MFE and magnitude of the magnetic field corresponding to one-half of the saturation value of MFE ($B_{1/2}$) support the fact that hyperfine mechanism plays the primary role. Quenching of MFE in the presence of gadolinium ions confirms that the radical pair is located near the micellar interface. MFE study has been further extended to protein-like bovine serum albumin in micellar solution. The results indicate loss in mobililty of radical pairs in the protein surfactant complex.

Introduction

Photoinduced electron-transfer or hydrogen-abstraction reactions involving aromatic carbonyl compounds have been well studied in the past. These reactions proceed via spin-correlated radical pair intermediates, and thus, the rates and yields of the reactions are susceptible to change in the presence of an external magnetic field. The radical ion pairs/radical pairs (RIP/RP) which are initially generated in the spin-correlated state can diffuse out to such an extent where the exchange interaction is negligible and interconversion between singlet (S_0) to all three degenerate triplet (T_{+1}, T_{-1}, T_0) spin states is possible by means of hyperfine interaction (HFI). The singlet correlated RIP/RP undergo geminate recombination, while for the RIP/RP in the triplet state a spin inversion or spin rephasing must occur before they can recombine. Consequently, the triplet born radical has a tendency to escape from the cage. However, in the presence of an external magnetic field if the Zeeman splitting is large enough to exceed the hyperfine width the degeneracy between the singlet and the triplet states is lifted. This affects the frequency of S $\leftrightarrow$ T interconversion and hence the population ratio of the singlet and triplet RIP/RP. Thus, analysis of MFE provides information on the dynamics and kinetics of the RP reaction. The magnetic field effect (MFE) on RIP/RP reactions depends not only on the spin evolution but also on the spatial evolution of the RIP/RP. It has been well established that the extent of MFE increases in the presence of micelles, particularly in the case of neutral RP. Micellar cage reduces the escape probability and hence increases the RIP/RP lifetime compared to that in homogeneous medium. MFE on triplet radical pairs produced by either photoelectron transfer or H-atom transfer from the detergent or some hydrogen donors in micelles, reverse micelles and other supercages has been extensively studied by several groups.[1−5]

Photoreduction efficiency of carbonyls has been found to be dependent on the electronic configuration of the lowest triplet state.[6,7] Thioxanthone (TX) has a lowest π,π^* triplet state at 65.5 kcal/mol.[8] The π,π^* state of aromatic ketones has been found to be less reactive toward benzylic and aliphatic hydrogen abstraction compared to that of the $n\pi^*$ state. The triplet state of TX and its derivatives has been well characterized in solvents of various polarities.[9,10] The energy of the triplet−triplet (T−T) absorption has been found to be dependent on the solvent polarity as well as on the substitution of TX. Triplet TX in the presence of amines has been found to act as an efficient cationic photoinitiator in radical polymerization and thus has found extensive use in various industrial applications.[11] TX derivatives are especially useful in surface-coating applications and varnishes which are curable by radiation-initiated polymerization. Other uses include offset lithographic ink and screen printing. Its photosensitizing activity is effective in treatment against solid tumors. Due to its antitumor activity it has gained importance in drug development.[12−14] The mechanism of DNA damage by UVA radiation in the presence of TX has also been investigated.[15] Photoexcited TX has been found to induce nucleotide oxidation in DNA through electron transfer. Moreover, protein damage induced by triplet TX has been investigated in order to elucidate the mechanism involved during destruction of tumors by TX.[16]

The present work involves investigation of MFE on the photoinduced electron-transfer reaction between TX and various electron donors like indoles (InH) and phenols (PhOH). The work has been further extended with amino acids and protein-like bovine serum albumin (BSA). Biological effects due to an external magnetic field have been a subject of interest in the recent past and well understood in terms of the radical pair mechanism (RPM). An external magnetic field has been found to influence photosynthetic reactions and different enzyme-mediated reactions by altering the radical pair recombination rate.[17,18] Models based on RPM have been proposed by Scaiano

* To whom correspondence should be addressed. Phone: +91 33 2473 3073. Fax: +91 33 2473 2805. E-mail: pcdnn@iacs.res.in.

10.1021/jp806880s CCC: $40.75
Published on Web 10/29/2008

et al., which shows that the average concentration of the radical pair increases in the presence of an external magnetic field and thus enhances the probability of radical reaction with cellular components.[19] In the same way, free-radical-induced reaction of proteins or DNA can thus be influenced by an external magnetic field. Our work aims to throwing light into the possibility of influencing TX radical-initiated reactions particularly with biologically relevant molecules in the presence of a magnetic field. Moreover, investigation of MFE in BSA−SDS complex provides insight into the nature of the interaction between proteins and surfactants.

Materials and Methods

Thioxanthone (TX), indole (InH) and 3-methylindole (3MInH) were obtained from Fluka and used after recrystallization from ethanol. Phenol (PhOH), *p*-cresol, tryptophan (TrpH), tyrosine (TyrH) and bovine serum albumin (BSA) were received from SRL and used without further purification. Purest grade SDS was received from SRL. Gd^{3+} and La^{3+} chlorides were received from Aldrich and used without further purification. Triply distilled deionized water was used for solution preparation. All solutions were deaerated by purging with argon for 30 min. The concentration of TX was maintained at 4×10^{-4} M, and that of the quencher unless otherwise stated was maintained at 2×10^{-3}M.

The experiments were carried out in a conventional laser flash photolysis (LFP) setup (Laser Kinetic Spectrometer, Applied Photophysics) coupled with an electromagnet. The low field ($B \leq 3$ kG) is provided by powering a Ferrite electromagnet with a DC source (30 V, 5A). For high-field studies, a pulsed magnetic field was used. A high-voltage capacitor (1000 μF, 4 kV) was charged to varying voltage and discharged by an ignitron through a pair of Helmholtz coils. A maximum field on the order of 5 T was obtained. The field was almost constant over the time of observation of the transient absorption of RIP (20 μs). The magnetic field was calibrated using the surgecoil technique. For the LFP studies, the third harmonic (355 nm) of a Nd:YAG laser (DCR-11, Spectra Physics) was employed as the pump source and a 250 W pulsed xenon lamp as the monitoring source. The photomultiplier (1P28) output was fed into a Tektronix oscilloscope (TPS 2012, 100 MHz, 1 GS/s), and the data was transferred to a computer using TekVISA software. The transient signal at each wavelength was averaged over 10 shots. The software Origin 6.1 was used for curve fitting. No degradation of the samples was observed during the experiment.

Theoretical calculations have been performed using the Gaussian 03 suite of the program.[20] The gas-phase geometry of the neutral radicals corresponding to both acceptor and donor molecules have been optimized using density functional theory (DFT). Calculations have been carried out at the UB3LYP/6-311++g** level. All optimized structures have been frequency checked.

Results and Discussions

Transient Absorption and MFE in SDS Micelle in the Absence of Quencher. Figure 1 shows the transient absorption spectra of TX in 0.2 M SDS micellar solution monitored at a 1 μs delay after irradiation with 355 nm. The spectra show absorption bands centered around 320, 430, and 600 nm. The absorption bands at 320 and 600 nm are much stronger compared to that at 430 nm. The time-resolved absorption spectrum of TX in solvents of different polarity has been reported previously.[10] The peak at 600 nm has been assigned to triplet TX, and that at 430 nm is due to the TX ketyl radical ($TXH^{\bullet}$) formed by hydrogen abstraction, while the absorption at 320 nm arises due to both the triplet TX and $TXH^{\bullet}$. In SDS micelle the relative absorption at 430 nm is weak compared to that at 600 and 320 nm, which is similar to that obtained in aprotic solvent. This indicates a lesser extent of hydrogen abstraction and hence a low population of $TXH^{\bullet}$ in micelles. TX, being insoluble in water, is expected to reside within the micelles. The polarity surrounding the TX in SDS micellar solution could be estimated by comparing the spectra in SDS micelle with those obtained in homogeneous solvents. Transient absorption spectra of TX in homogeneous solvents of varying polarity show that the peak corresponding to the triplet TX is blue shifted with increasing solvent polarity.[10] The triplet absorption peak near 600 nm in micelles indicates that that the dielectric constant surrounding the TX is close to 33, i.e., TX resides near the stern layer of the micelles and neither in the hydrocarbon micellar interior where the dielectric constant is too low nor within the bulk water where the dielectric constant is much higher. Similar results have been reported in the case of derivatives of TX in SDS micellar solutions.[21] Incorporation of radical pairs within the micelles elongates the lifetime of the RP and hence amplifies the extent of MFE. However, transient absorption spectra of TX in SDS micelle in the presence of a magnetic field exhibit no appreciable MFE. The lowest triplet state of TX being π,π^* in character is less reactive toward hydrogen abstraction from the micellar backbone, and this may result in a low concentration of ketyl radical in the medium. We conclude that as $TXH^{\bullet}$ is low in concentration the extent of MFE is too small to be detected. A similar absence of MFE has been previously reported in the case of benzophenone in the cetyltrimethylammonium bromide RP system.[22] The results have been accounted for in terms of the poor hydrogen-donating ability of the micellar aliphatic chain.

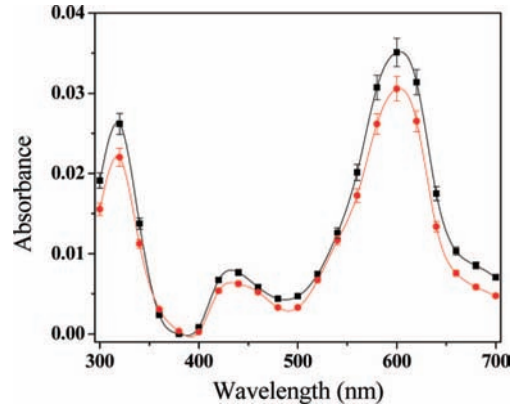

Figure 1. Transient absorption spectra of 4×10^{-4} M TX in 0.2 M SDS obtained at (■) 1 and (●) 8 μs delay after pulse irradiation.

TABLE 1: Quenching Constant (k_q) of $^3TX^*$ by Different Quencher in 0.2 M SDS Micelle

donor	k_q (M^{-1} s^{-1})
InH	$2.14 (\pm 0.2) \times 10^9$
3MInH	$1.07 (\pm 0.4) \times 10^9$
PhOH	$2.84 (\pm 0.15) \times 10^9$
p-cresol	$1.80 (\pm 0.05) \times 10^9$
TrpH	$2.26 (\pm 0.12) \times 10^9$
TyrH	$1.38 (\pm 0.2) \times 10^9$
BSA	$5.20 (\pm 0.2) \times 10^8$

Transient Absorption and MFE in the Presence of InH and 3MInH. Addition of a quencher like indoles and phenols results in quenching of the triplet TX. The rate constant for the

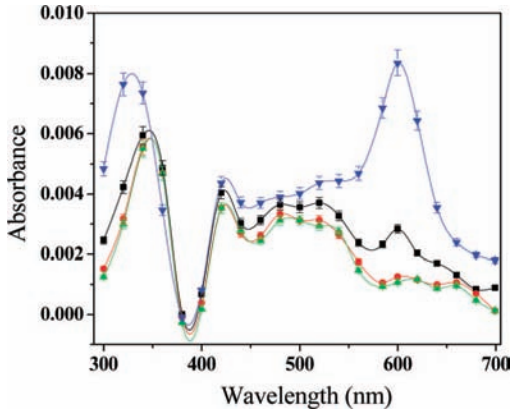

Figure 2. Transient absorption spectra of 4×10^{-4} M TX and 2×10^{-3} M InH in 0.2 M SDS obtained at (▼) 400 ns, (■) 1 μs, (●) 5 μs, and (▲) 8 μs delay after pulse irradiation.

TABLE 2: Variation of Rate Constants (k_f) and Escape Radical Yield with External Magnetic Field in 0.2 M SDS Solution

	$k_f \times 10^6$ (s^{-1})		
quencher	$B = 0$ mT	$B = 0.7$ mT	$[(Y(B) - Y(0))/Y(0)] \times 100$ measured at 420 nm after 8 μs of 355 nm pulse, %
InH	4.25	1.77	64.9
3MInH	3.98	1.69	87.8
PhOH			10.5
p-cresol			35.03
TrpH			19.5
TryH			7.4
BSA	1.49	0.91	46.7

quenching reaction of triplet TX with different quenchers has been measured at 600 nm and is listed in Table 1. The quenching constants have been experimentally determined by measuring the slope of the Stern Volmer relation

$$\tau^{-1} = \tau_o^{-1} + k_q[Q] \quad (1)$$

where τ_o^{-1} and τ^{-1} are the reciprocal of the triplet state lifetime in the absence and presence of quencher (Q) and k_q is the quenching constant. The transient absorption spectra of TX in SDS micelle in the presence of InH and 3MInH has been monitored at different time delays after the laser flash (Figure 2). The absorption spectra recorded at short time delay (400 ns) after the laser pulse show distinct peaks at 320, 420, and 600 nm. With increasing time delay the intensity of the triplet absorption band at 600 nm gradually diminishes and becomes much weaker compared to the absorption of the $TXH^{\bullet}$ and thus indicates quenching of triplet TX. It is to be noted that the ratio of the absorption intensity at 420 and 600 nm at 8 μs time delays (where the radical absorption is prominent) is higher in the presence of quencher compared to that in the absence of quencher. This indicates formation of a substantial amount of $TXH^{\bullet}$ in the presence of quencher. Triplet InH is known to absorb near 430 nm. However, the energy transfer from triplet TX to InH or 3MInH is unlikely to occur as the triplet energy level of InH (70.76 kcalmol^{-1}) and 3MInH (68.19 kcal mol^{-1})[23] is much higher than that of TX (65.5 kcal mol^{-1}). An analysis of the decay profile at 320 and 420 nm reveals that there is a long time residual absorption. The decay at these wavelengths is biexponential in nature and follows the expression $A(t) = I_f \exp(-k_f t) + I_s \exp(-k_s t)$, where k_f and k_s are the rate constants for the fast and slow components of the decay profiles, respectively. The fast component corresponds to decay due to

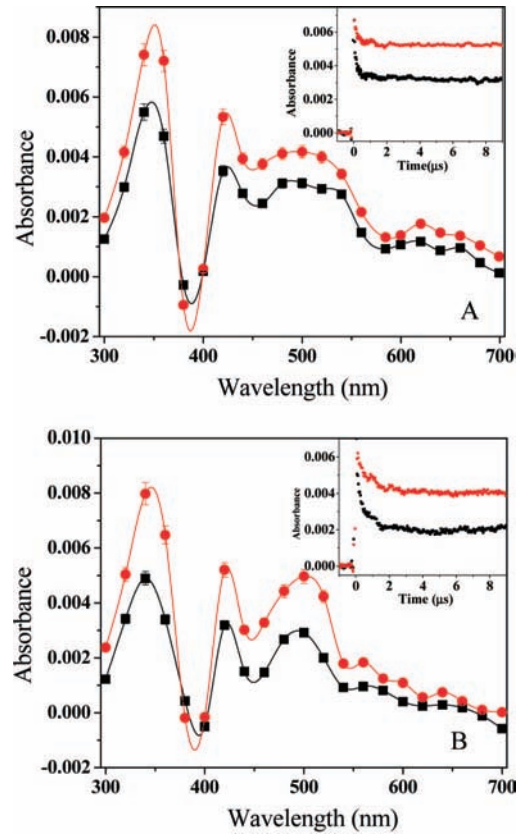

Figure 3. Transient absorption spectra of TX (4×10^{-4} M) and (A) InH (2×10^{-3} M) and (B) 3InH (2×10^{-3} M) in 0.2 M SDS, obtained at a 8 μs delay after a 355 nm laser pulse in the presence of a magnetic field of (■) 0 and (●) 0.7 mT. (Inset) Decay profile for (■) 0 and (●) 0.7 mT at 420 nm.

the geminate recombination, while the slow component corresponds to the escape radical. No such residual absorption has been observed at 600 nm, which indicates the absence of radical in this region. Additionally, a broad hump develops near 500 and 640 nm. The band near 640 nm has been previously assigned to the TX anion ($TX^{-\bullet}$) generated by electron transfer from the quencher.[24] TX triplet is known to undergo an electron-transfer reaction with electron-donor-like amines, InHs, to form $TX^{-\bullet}$, which subsequently abstracts hydrogen to form $TXH^{\bullet}$.[21,24] The fact that the absorption at 640 nm is negligible compared to that at 420 nm suggests that the electron transfer is followed by a proton transfer and hence the population of the neutral radical is relatively much higher than that of the anion. The band near 500 nm may be assigned to $In^{\bullet}$ radical, which is formed as a result of proton abstraction by $TX^{-\bullet}$ and known to absorb near 520 nm as evident from earlier investigations.[25]

Application of a magnetic field on the radical ion pair within micelles has been extensively studied in the past. For radical pairs initially produced in the singlet state the presence of a magnetic field enhances the singlet yield while the triplet product yield enhances in the case of radical pairs generated from triplet precursors. In the present case, application of a magnetic field results in a decrease in k_f with a simultaneous increase in the escape yield at long time delay, which supports the fact that the radical pair is generated from the triplet state (Table 2). The extent of MFE is found to be maximum near 420 nm, where $TXH^{\bullet}$ absorbs predominantly (Figure 3). Near 600 nm, where the TX triplet absorbs, there is a small extent of MFE. Thus, in the present case the following reaction scheme can be proposed.

$$TX \xrightarrow{h\nu} {}^1TX^* \rightarrow {}^3TX^* \quad (2)$$

$${}^3TX^* + InH \rightarrow {}^3(TX^{\bullet -}InH^{\bullet +}) \text{ electron transfer} \quad (3)$$

$${}^3(TX^{\bullet -}InH^{\bullet +}) \xrightarrow[HFI]{MFE} {}^1(TX^{\bullet -}InH^{\bullet +}) \quad (4)$$

$${}^1(TX^{\bullet -}InH^{\bullet +}) \rightarrow TX + InH \text{ cage product} \quad (5)$$

$${}^3(TX^{\bullet -}InH^{\bullet +}) \rightarrow \text{escape product} \quad (6)$$

$${}^3(TX^{\bullet -}InH^{\bullet +}) \rightarrow {}^3(TXH^{\bullet}In^{\bullet}) \text{ proton transfer} \quad (7)$$

$${}^3(TXH^{\bullet}In^{\bullet}) \xrightarrow[HFI]{MFE} {}^1(TXH^{\bullet}In^{\bullet}) \quad (8)$$

$${}^1(TXH^{\bullet}In^{\bullet}) \rightarrow TX + InH \text{ cage product} \quad (9)$$

$${}^3(TXH^{\bullet}In^{\bullet}) \rightarrow \text{escape product} \quad (10)$$

Transient Absorption and MFE in the Presence of Phenol and *p*-Cresol. The time-resolved transient absorption spectra of TX have been monitored in the presence of quenchers like PhOH and *p*-cresol. Figure 4 shows the absorption spectra measured 8 μs after the laser flash. The decrease in the peak intensity at 600 nm and generation of the band at 420 nm suggests that in the presence of PhOH or *p*-cresol triplet TX gets quenched rapidly with a simultaneous production of the $TXH^{\bullet}$. PhOH is known to be a good hydrogen donor compared to InH. Detailed investigations involving the quenching of the aromatic ketones by phenol and its derivatives has been carried out earlier.[26,27] Quenching of aromatic ketones with n,π^* triplet by PhOH has been rationalized in terms of formation of a charge-transfer complex followed by a proton transfer, while hydrogen abstraction from PhOH by carbonyls having a π,π^* triplet excited state is known to involve an electron transfer within the hydrogen-bonded exciplex between the triplet carbonyl and PhOH. Formation of this hydrogen-bonded exciplex effectively lowers both the reduction potential of the acceptor and the oxidation potential of the donor (PhOH) and favors the process of electron transfer. The electron transfer is followed by proton transfer, which finally yields the neutral radical pair. TX possesses a lowest π,π^* triplet excited state and is known to abstract hydrogen from phenol via formation of the hydrogen-bonded complex. Thus, the interaction of TX with phenols can be represented by the following mechanism

$${}^3TX^* + PhOH \xrightarrow{h\nu} {}^3TX^* \cdots PhOH$$

hydrogen-bonded complex (11)

$${}^3TX^* + PhOH \rightarrow {}^3(TX^{\bullet -}PhOH^{\bullet +}) \text{ electron transfer} \quad (12)$$

$${}^3(TX^{\bullet -}PhOH^{\bullet +}) \xrightarrow[HFI]{MFE} {}^1(TX^{\bullet -}PhOH^{\bullet +}) \quad (13)$$

$${}^1(TX^{\bullet -}PhOH^{\bullet +}) \rightarrow TX + PhOH \text{ cage product} \quad (14)$$

$${}^3(TX^{\bullet -}PhOH^{\bullet +}) \rightarrow {}^3(TXH^{\bullet}PhO^{\bullet}) \text{ proton transfer} \quad (15)$$

$$3(TX^{\bullet -}PhOH^{\bullet +}) \rightarrow \text{escape product} \quad (16)$$

$${}^3(TXH^{\bullet}PhO^{\bullet}) \xrightarrow[HFI]{MFE} {}^1(TXH^{\bullet}PhO^{\bullet}) \quad (17)$$

$${}^1(TXH^{\bullet}PhO^{\bullet}) \rightarrow TX + PhOH \text{ cage product} \quad (18)$$

$${}^3(TXH^{\bullet}PhO^{\bullet}) \rightarrow \text{escape product} \quad (19)$$

It is to be mentioned that $PhO^{\bullet}$, which absorbs in the region near 385−405 nm, cannot be identified distinctly in the present case. A small shoulder appears near 380 nm. The absence of the $PhO^{\bullet}$ band may be due to the overlap of the $TXH^{\bullet}$ absorption band near 420 nm. However, laser flash photolytic experiments in aerated solution exhibits a peak near 400 nm which may be due to $PhO^{\bullet}$. The appearance of the $PhO^{\bullet}$ band may be accounted for in terms of the low reactivity of $PhO^{\bullet}$ toward oxygen compared to that of ketone triplets and ketyl radicals.[28,29]

MFE on the yield of escape radicals has been measured. However, the change in the yield of TX escape radical in the presence of PhOH has been found to be comparatively lower than that noted for the InH derivatives. The triplet yields in the presence of MF are provided in Table 2. The lower extent of MFE in phenolic derivatives may be explained in terms of the reduced efficiency of geminate ${}^3(TXH^{\bullet}PhO^{\bullet})$ formation.[30] The lesser extent of radical formation is due to the reverse electron transfer within the geminate pair ${}^3(TX^{\bullet -}PhOH^{\bullet})$ or nonproductive collapse of the exciplex to the ground-state ketone and PhOH by intersystem crossing.

Transient Absorption and MFE in the Presence of Amino Acids. Figure 5 shows the transient absorption spectra of TX in the presence of amino acids like TrpH and TyrH in 0.2 M SDS micelle monitored at a 8 μs delay after the laser flash. The absorption spectra indicates quenching of triplet TX with simultaneous formation of $TXH^{\bullet}$ in the presence of amino acids. In addition, a broad band appears in the region 460−520 nm in the case of TrpH, which is due to the $Trp^{\bullet}$ radical that absorbs near 510 nm.[31] However, $TyrH^{\bullet}$, which is known to absorb near 410 nm, is not very prominently detected in our case. This may

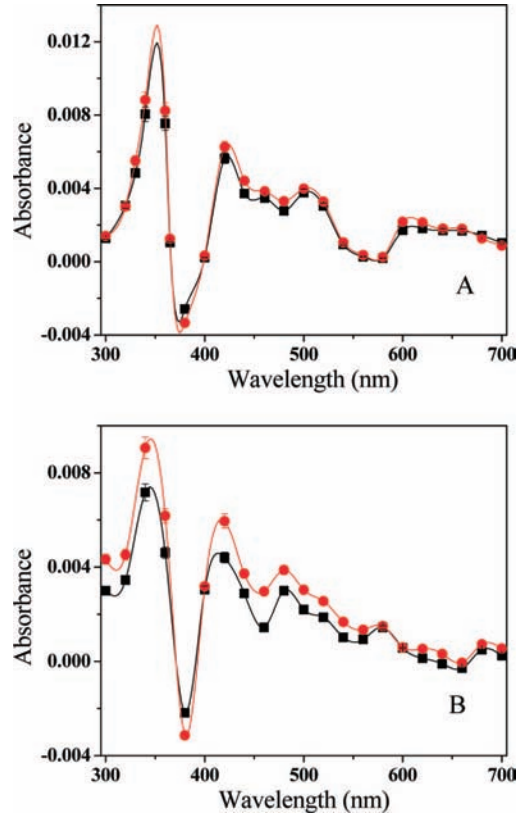

Figure 4. Transient absorption spectra of 4×10^{-4} M TX and 2×10^{-3} M (A) PhOH and (B) *p*-cresol in 0.2 M SDS, obtained at a 8 μs delay after a 355 nm laser pulse in the presence of a magnetic field of (■) 0 and (●) 0.7 mT.

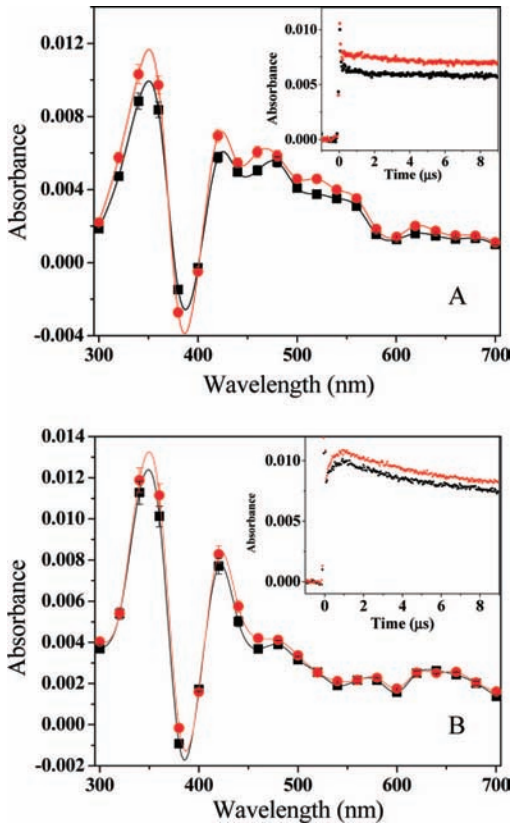

Figure 5. Transient absorption spectra of 4×10^{-4} M TX and (A) TrpH (2×10^{-3} M) and (B) TyrH (2×10^{-3} M) in 0.2 M SDS micellar solution, obtained at a 8 μs delay after a 355 nm laser pulse in the presence of a magnetic field of (■) 0 and (●) 0.7 mT. (Inset) Decay profile for (■) and (●) 0.7 mT at 420 nm.

be due to the overlap of the absorption band of $TXH^{\bullet}$ at 420 nm. In fact, the decay profile at 420 nm shows growth in the presence TryH (Figure 5B, inset), which indicates formation of $Try^{\bullet}$. Thus, the transient absorption spectra resulting in the presence TrpH and TyrH can be explained on the basis of a mechanism involving electron transfer between TX and the amino acids producing radical ion pairs ($TX^{\bullet -}$ and $Trp^{\bullet +}$). Electron transfer is followed by proton abstraction by the $TX^{\bullet -}$ that finally generates the neutral radical pairs. In fact, previous laser flash photolytic studies involving different derivatives of TX in the presence of amino acids like TrpH and TyrH also indicated the occurrence of an electron-transfer coupled proton-transfer reaction whereby neutral $Trp^{\bullet}$ and $Tyr^{\bullet}$ radicals are generated.[16] MFE on the radical pairs generated by the reaction between triplet TX and amino acids have been monitored. The observed MFE, though small, indicates formation of radical pairs due to the reaction between TX and amino acids. Small MFE indicate the low extent of proton transfer from the amino acids which may be attributed to the steric effect due to the bulky size of the amino acids that restricts proton abstraction by TX. Nevertheless, such MFE in the presence of TrpH and TyrH implies the possibility of influencing various catalytic and enzymatic reactions involving radicals of amino acids.

The decays obtained at 420 nm for various donors have been monitored at varying external magnetic fields up to 2 T. The escape product yield at longer times (8 μs) plotted against strength of the magnetic field shows that MFE increases with increasing field. The MFE saturates at nearly 100 G and shows no change even at very high field. Figure 6 represents the escape product yield for InH, 3MInH, TrpH, and BSA at different magnetic field strength. The magnetic field corresponding to one-half of the saturation value of MFE ($B_{1/2}$) has been found and is presented in Table 3. It is to be mentioned that the low extent of MEF causes difficulty in monitoring the $B_{1/2}$ value for phenolic derivatives. MFE on triplet radical pairs has been explained in terms of Δg, hyperfine coupling and relaxation mechanism. In the range of low magnetic field the dominant mechanism is HFC, while the Δg mechanism and relaxation mechanism operate at high magnetic field strength. Our observation of saturation of MFE in the low-field range and subsequent absence of further changes in the extent of MFE suggests that the hyperfine mechanism is operative in the present case and excludes the possibility of a Δg mechanism and relaxation mechanism. Moreover, the $B_{1/2}$ values are consistent with the hyperfine mechanism. However, it is to be mentioned that the $B_{1/2}$ values determined experimentally are not very accurate.

$B_{1/2}$ values have been calculated theoretically. The gas-phase geometry of the neutral radicals corresponding to both acceptor and donor molecules have been optimized using DFT at the UB3LYP/6-311++g** level. The hyperfine coupling constants (α) thus obtained from the Gaussian output file were used to calculate $B_{1/2}$ values according to the following formula[32]

$$B_{1/2} = \frac{2(B_m^2 + B_n^2)}{B_m + B_n} \tag{20}$$

where

$$B_r^2 = \sum_i^r I_i(I_i + 1)a_i^2 \tag{21}$$

($r = m$ and n; i represents every nuclear spin in a radical) Further the natural abundance of various isotopes has been taken into account, and thus, the equation has been modified as

$$B_r^2 = \sum_i^r [I_i(I_i + 1)a_i^2]N_i \tag{22}$$

where N_i represents the respective abundance of different isotopes.

The experimental value has been found to be much higher than the calculated values. Deviation in experimental and calculated $B_{1/2}$ values in the case of RIP has been previously accounted for in terms of an electron-hopping mechanism and lifetime broadening.[33] However, a similar explanation could not be extended in the present case, which involves neutral radicals.

The extent of MFE has been monitored in the presence of Gd^{3+} ions. The location of the radical pairs inside the SDS micelle has been probed in the presence of Gd^{3+} ions. Gd^{3+} ions have unpaired electrons and are paramagnetic and thus capable of quenching the MFE. Gd^{3+} ions remain distributed in aqueous bulk and are also adsorbed on the micellar surface of the SDS micelle. Adsorption of Gd^{3+} ions on the micellar interface MFE has been probed through MFE studies on pyrene DMA exciplexes.[34] The ions in the aqueous phase are unable to quench the MFE, while those at the micellar interface will interact with the radical pairs. In the present work MFE monitored at 420 nm has been found to be quenched when Gd^{3+} ions are added to the aqueous micellar medium (Figure 7). TX and the InH derivatives both being insoluble in water are expected to remain within the hydrophobic interior of the micelle. The radical ion pairs formed after electron transfer between the triplet TX and the quencher are charged dipolar species which preferably remain near the micellar head groups rather than in the micellar interior. Quenching of MFE at 420

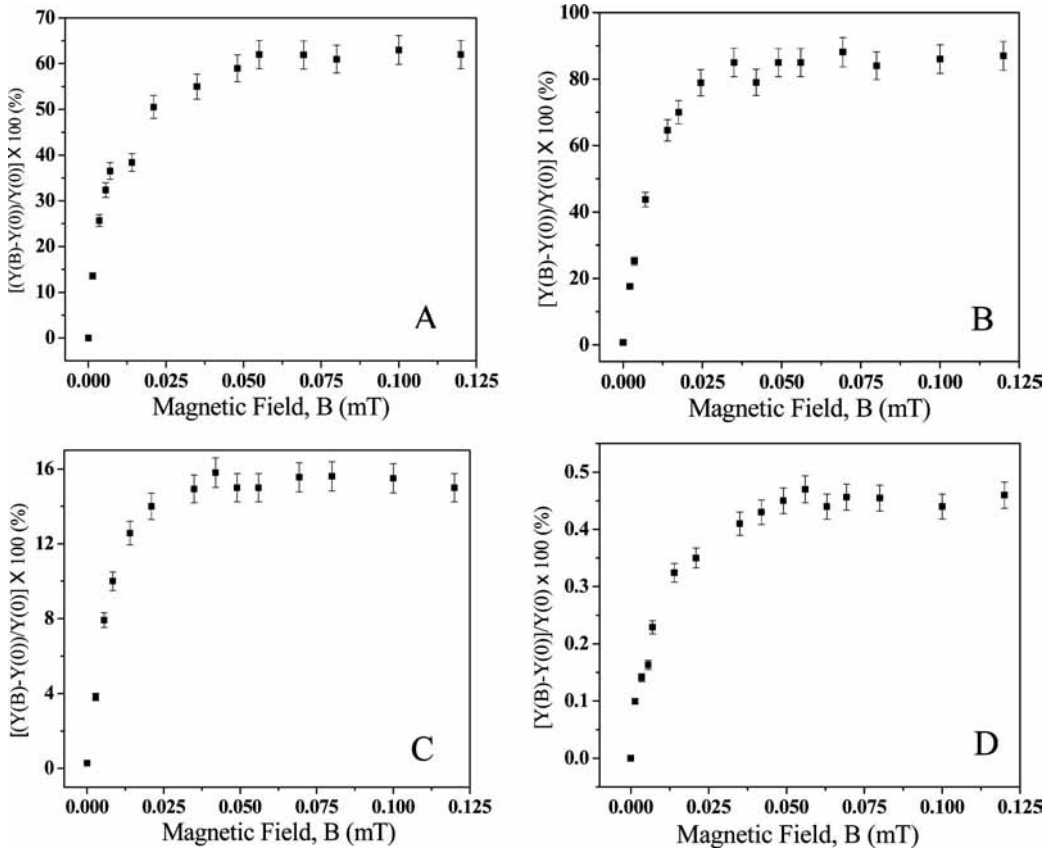

Figure 6. Plot of escape yield, $[Y(B) - Y(0)]/Y(0)$, at 420 nm as a function of external magnetic fields in the presence of (A) InH, (B) 3MInH, (C) TrpH, and (D) BSA in deaerated SDS micellar solution.

TABLE 3: Experimental and Calculated $B_{1/2}$ Values for TX and Various Donor Molecules

donor	$B_{1/2}$(exp), G[a]	$B_{1/2}$(calcd), G
TXH•In•	58.7	21.95
TXH•3MIn•	76.7	50.81
TXH•PhO•		20.20
TXH•*p*-Cresol		35.39
TXH•Trp•	56.1	22.58
TXH•Try•		20.56
TXH•BSA•	81.3	

[a] Standard deviation in experimental $B_{1/2}$ measurement is ±12 G.

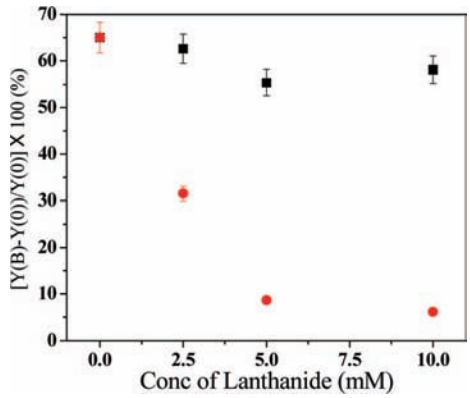

Figure 7. Variation of MFE in TX-InH with a concentration of (●) Gd^{3+} and (■) Ln^{3+} ions.

nm in the presence of Gd^{3+} ions indicates that the neutral radical pairs formed thereafter due to proton transfer interact with the Gd^{3+} adsorbed on the micellar surface. This confirms the location of the neutral radical pair near the micellar interface.

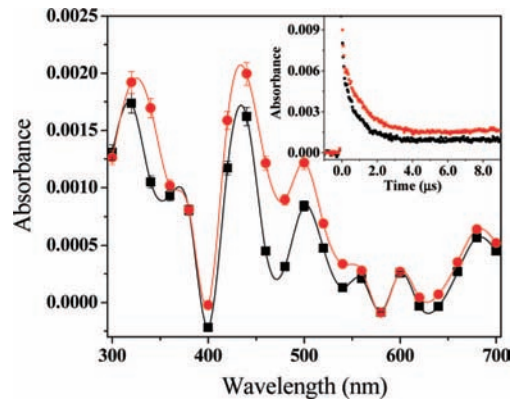

Figure 8. Transient absorption spectra of TX (4×10^{-4} M) and BSA (6×10^{-4} M) in 0.2 M SDS, obtained at a 8 μs delay after a 355 nm laser pulse in the presence of a magnetic field of (■) 0 and (●) 0.7 mT. (Inset) Decay profile for (■) 0 and (●) 0.7 mT at 420 nm.

In order to confirm that the decrease in MFE is not because of the charge of the ions or structural modification of micelles due to adsorption of ions the MFE experiments have been repeated with diamagnetic La^{3+} ions having no unpaired electrons. In the presence of La^{3+} MFE monitored at 420 nm is found to remain unaffected (Figure 7).

Transient Absorption and MFE in a BSA Environment. This work has been further extended to study the interaction of triplet TX with model protein BSA. Figure 8 shows the transient absorption spectra of TX in the presence of 6×10^{-4} M BSA in 0.2 M SDS irradiated with a 355 nm laser pulse. The appearance of the absorption peak at 420 nm indicates formation of TXH•. BSA contains TrpH and TyrH residues within its chain which can interact with triplet TX. A closer look at the decay

profiles at 420 nm in the presence of BSA reveals that the yield of the escape radicals at longer delay times is much less compared to that obtained for free amino acids. The rate constant for the fast decaying component has been found to be much slower than that obtained in the case of free donor like InH. While for free InH $k_f \approx 4.25 \times 10^6\ s^{-1}$, the k_f value for BSA is $\sim 1.49 \times 10^6\ s^{-1}$ (Table 2.). This in turn indicates a slower recombination yield in BSA environment.

Detailed investigations have revealed that BSA interacts with anionic surfactants like SDS and forms a protein−surfactant complex which finally leads to unfolding of the protein. [35−38] The binding isotherm of SDS with BSA contains four distinct regions. Initially at low concentration of SDS the surfactant molecules bind to the specific high-energy sites of the protein. On increasing the surfactant concentration a noncooperative binding starts which is followed by cooperative binding of the SDS molecules to the protein. Such cooperative association of the surfactant molecules results in formation of micelle-like clusters that remain adhered to the polypeptide chain. At a sufficiently high concentration the binding reaches saturation after which any further rise in surfactant concentration results in formation of free micelle that coexists with the protein-bound micelles. Earlier investigation shows that the saturation binding of SDS to BSA corresponds to 1.35 g of SDS /1 g of BSA at low ionic strength.[39] This has been further confirmed by fluorescence studies.[35,36] In the present case the molar ratio of concentration of SDS and BSA, i.e., [SDS]/[BSA], that has been employed implies that the experiment has been carried out at the saturated region of the binding isotherm where the BSA remains in an unfolded condition. Fluorescence, ESR, and NMR studies on BSA in the presence of SDS revealed that near the saturation region the unfolded protein wraps around the periphery of the micelles giving rise to the necklace bead structure.[35,36] The surroundings of the TrpH residues have been found to become more hydrophobic with gradual addition of surfactant molecules as indicated by the blue shift in the emission spectra of the intrinsic TrpH residues.[40] Such increase in hydrophobicity around the TrpH residues is due to binding of the surfactant molecules near the TrpH site of BSA. The TX molecules within the SDS micelles thus interact with the amino acids residue toward the peripheral surface of the micelles. However, in the case of BSA as the quencher, diffusion of the constituent radicals in the radical pair is hindered as the donor remains bound to the protein chain. Moreover, NMR and fluorescence quenching studies have established that the mobility of the micellar headgroup becomes restricted in the protein−surfactant complex.[35,41] Thus, the radical pairs formed in this region cannot diffuse out easily to form the escape product. This results in the low yield of escape radicals in the BSA environment as is evident from the weak residual absorption at longer time delay. The restricted mobility of the molecules near the stern layer of the SDS micelles in the presence of BSA chain may be also considered to be the cause behind the lowering of the quenching rate constant in BSA−SDS micellar solution compared to that for free donors. In the BSA−SDS complex efficient electron transfer between the acceptor and the donor molecules gets hindered. In fact, translational diffusion coefficients of various coumarin dyes have been found to become slower in the BSA−SDS complex compared to that in the free micelle,which have been determined to be the cause for the slower electron-transfer rate in the protein−surfactant complex. Thus, unlike that in free micelles where the quencher could easily diffuse and move toward the acceptor, the quenching rate of the triplet TX is lowered in the BSA−SDS complex due to the hindered diffusion in the BSA−SDS complex. Also, the fact that the donor is bound to the BSA chain may contribute to the difficulty in attaining the appropriate condition for the electron transfer which in turn is reflected in the quenching constant magnitude.

Application of MF in the presence of BSA results in an increase in the triplet yield. This implies that similar to the case of pure micelles the lifetime of the geminate radical pairs within the BSA−SDS complex is sufficiently long for the spin reversal to take place. MFE on radical pairs generated in a protein environment in the absence of any external denaturing agent has been reported earlier.[42,43] The MFE observed for benzophenone in the presence of BSA and human serum albumin suggests poor confinement of the radical pair within the protein environment. On the other hand, the Coulombic attraction has been identified to play a role in the manifestation of MFE in the case of hen egg white lysozyme. The considerable extent of MFE in the present case suggests that the population of geminate radical pairs is quite high in BSA−SDS complex unlike that reported earlier in the case of 4-nitroquinoline-1-oxide and InH derivatives in a protein environment. However, previous studies involving proteins like BSA and lysozyme with organic molecules suggested that the TrpH residues, rather than TyrH, participate in the photoinduced electron-transfer reaction. Such conclusions have been drawn on the basis of the resemblance of the transient spectra in BSA environment to that of free TrpH. Our results however do not clearly indicate which of the amino acid residues preferentially interact with the TX molecule.

Conclusions

This work describes the MFE on radical pairs generated in SDS micellar medium on photoexcitation of TX in the presence of indoles and phenols. The photoinduced electron-transfer reaction is followed by proton transfer. The yield of the free radicals has been found to increase considerably with magnetic field. The extent of MFE has been found to differ for various donors and explained in terms of a hyperfine coupling mechanism. The radical pairs generated distributes primarily toward the periphery of the micelles. Our MFE results in the presence of amino acids and protein-like BSA explore the possibility of investigation and application of a radical pair mechanism in biological systems. However, the dynamics of the radical pairs have been found to slow down in the BSA−SDS complex compared to that in pure SDS micelle.

Acknowledgment. D.D. thanks the Council of Scientific and Industrial Research (CSIR), India, for awarding a senior research fellowship. We thank Professor S. P. Bhattacharyya of our department for helpful discussion on theoretical calculations. We also thank the reviewers for important suggestions.

References and Notes

(1) Steiner, U. E.; Ulrich, T. *Chem. Rev.* **1989**, *89*, 51.
(2) Nagakura, S., Hayashi, H., Azumi, T., Eds. *Dynamic Spin Chemistry*; Kodansha/Wiley: Tokyo/New York, 1998.
(3) Choudhury, S. D.; Basu, S. *J. Phys. Chem. A* **2005**, *109*, 8113.
(4) Akimoto, Y.; Fujiwara, Y.; Tanimoto, Y. *Chem. Phys. Lett.* **2000**, *326*, 383.
(5) Miura, T.; Maeda, K.; Arai, T. *J. Phys. Chem. A* **2006**, *110*, 4151.
(6) Dauben, W. G.; Salem, L.; Turro, N. J. *Acc. Chem. Res.* **1975**, *8*, 41.
(7) Salem, L. *J. Am. Chem. Soc.* **1974**, *96*, 3486.
(8) Dalton, J. C.; Montgomery, F. C. *J. Am. Chem. Soc.* **1974**, *96*, 6230.
(9) Yip, R. W.; Szabo, A. G.; Tolg, P. K. *J. Am. Chem. Soc.* **1973**, *95*, 4471.
(10) Ferreira, G. C.; Schmitt, C. C.; Neumann, M. G. *J. Braz. Chem. Soc.* **2006**, *17*, 905.

(11) Roffey, C. G. *Photopolymerisation of Surface Coatings*; Wiley, New York, 1982.
(12) Corbett, T. H.; Panchapor, C.; Polin, L.; Lowichik, N.; Pugh, S.; White, K.; Kushner, J.; Meyer, J.; Czarnecki, J.; Chinnukroh, S.; Edelstein, M.; LoRusso, P.; Heilbrun, L.; Horwitz, J. P.; Grieshaber, C.; Perni, R.; Wentland, M.; Coughlin, S.; Elenbaas, S.; Philion, R.; Rake, J. *Invest. New Drugs* **1999**, *17*, 17.
(13) Stevenson, J. P.; DeMaria, D.; Reilly, D.; Purvis, J. D.; Graham, M. A.; Lockwood, G.; Drozd, M.; O'Dwyer, P. J. *Cancer Chemother. Pharmacol.* **1999**, *44*, 228.
(14) Izbicka, E.; Lawrence, R.; Davidson, K.; Rake, J. B.; VonHoff, D. D. *Invest. New Drugs.* **1999**, *16*, 221.
(15) Hirakawa, K.; Yoshida, M.; Oikawa, S.; Kawanishi, S. *Photochem. Photobiol.* **2003**, *77*, 349.
(16) Zhu, H.; Wang, W.; Yao, S. *Invest. New Drugs.* **2006**, *24*, 465.
(17) Grissom, C. B. *Chem. Rev.* **1995**, *95*, 3.
(18) Chagovetz, A. M.; Grissom, C. B. *J. Am. Chem. Soc.* **1993**, *115*, 12152.
(19) Scaiano, J. C.; Cozens, F. L.; McLean, J. *Photochem. Photobiol.* **1994**, *59*, 585.
(20) Frisch, M. J. ; Trucks, G. W.; Schlegel, H. B.; Scuseria, G. E.; Robb, M. A.; Cheeseman, J. R. ; Montgomery, J. A., Jr.; Vreven, T.; Kudin, K. N. ; Burant, J. C.; Millam, J. M.; Iyengar, S. S.; Tomasi, J.; Barone, V.; Mennucci, B.; Cossi, M.; Scalmani, G.; Rega, N.; Petersson, G. A.; Nakatsuji, H.; Hada, M.; Ehara, M.; Toyota, K.; Fukuda, R.; Hasegawa, J.; Ishida, M.; Nakajima, T.; Honda, Y.; Kitao, O.; Nakai, H.; Klene, M.; Li, X.; Knox, J. E.; Hratchian, H. P.; Cross, J. B.; Bakken, V.; Adamo, C.; Jaramillo, J.; Gomperts, R.; Stratmann, R. E.; Yazyev, O.; Austin, A. J.; Cammi, R.; Pomelli, C.; Ochterski, J. W.; Ayala, P. Y.; Morokuma, K.; Voth, G. A.; Salvador, P.; Dannenberg, J. J.; Zakrzewski, V. G.; Dapprich, S.; Daniels, A. D.; Strain, M. C.; Farkas, O.; Malick, D. K.; Rabuck, A. D.; Raghavachari, K.; Foresman, J. B.; Ortiz, J. V.; Cui, Q.; Baboul, A. G.; Clifford, S.; Cioslowski, J.; Stefanov, B. B.; Liu, G.; Liashenko, A.; Piskorz, P.; Komaromi, I.; Martin, R. L.; Fox, D. J.; Keith, T.; Al-Laham, M. A.; Peng, C. Y.; Nanayakkara, A.; Challacombe, M.; Gill, P. M. W.; Johnson, B.; Chen, W.; Wong, M. W.; Gonzalez, C.; Pople, J. A. *Gaussian 03, revision B.04*; Gaussian, Inc.: Wallingford, CT, 2004.
(21) Fouassier, J. P.; Lougnot, D. J. *J. Appl. Polym. Sci.* **1987**, *34*, 477.
(22) Haldar, M.; Chowdhury, M. *Chem. Phys. Lett.* **1999**, *312*, 432.
(23) Wilkinson, F.; Garner, A. *J. Chem. Soc., Faraday Trans 2* **1977**, *73*, 222.
(24) Yates, S. F.; Schuster, G. B. *J. Org. Chem.* **1984**, *49*, 3349.
(25) Kasama, K.; Takematsu, A.; Aral, S. *J. Phys. Chem.* **1982**, *86*, 2420.
(26) Lathioor, E. C.; Leigh, W. J. *Photochem. Photobiol.* **2006**, *82*, 291.
(27) Leigh, W. J.; Lathioor, E. C.; Pierre, M. J. *J. Am. Chem. Soc.* **1996**, *118*, 12339.
(28) Perez-Prieto, J.; Bosca, F.; Galian, R. E.; Lahoz, A.; Domingo, L R.; Miranda, M. A. *J. Org. Chem.* **2003**, *68*, 5104.
(29) Bejan, E. V.; Font-Sanchis, E.; Scaiano, J. C. *Org. Lett.* **2001**, *3*, 4059.
(30) Das, P. K.; Encinas, M. V.; Scaiano, J. C. *J. Am. Chem. Soc.* **1981**, *103*, 4154.
(31) Galian, R. E.; Pastor-Perez, L.; Miranda, M. A.; Perez-Prieto, J. *Chem. Eur. J.* **2005**, *11*, 3443.
(32) Werner, H. J.; Staerk, H.; Weller, A. *J. Chem. Phys.* **1978**, *68*, 2419.
(33) Kruger, H. W.; Michel-Beyerle, M. E.; Knapp, E. W. *Chem. Phys.* **1983**, *74*, 205.
(34) Haldar, M.; Nath, D. N. *Chem. Phys. Lett.* **2004**, *387*, 81.
(35) Turro, N. J.; Lei, X.-G.; Ananthapadmanabhan, K. P.; Aronson, M. *Langmuir* **1995**, *11*, 2525.
(36) Vasilescu, M.; Angelescu, D.; Almgren, M.; Valstar, A. *Langmuir* **1999**, *15*, 2635.
(37) Valstar, A.; Vasilescu, M.; Vigouroux, C.; Stilbs, P.; Almgren, M. *Langmuir* **2001**, *17*, 3208.
(38) Shirama, K.; Tsujii, K.; Takagi, T. *J. Biochem.* **1974**, *75*, 309.
(39) Reynolds, J. A.; Tanford, C. *Proc. Natl. Acad. Sci. U.S.A.* **1970**, *66*, 1002.
(40) Gelamo, E. L.; Tabak, M. *Spectrochim. Acta A.* **2000**, *56*, 2255.
(41) Chakraborty, A.; Seth, D.; Setua, P.; Sarkar, N. *J. Phys. Chem. B* **2006**, *110*, 16607.
(42) Choudhury, S. D.; Basu, S. *J. Phys. Chem. B* **2006**, *110*, 8850.
(43) Mohtat, N.; Cozens, F. L.; Hancock-Chen, T.; Scaiano, J. C.; McLean, J.; Kim, J. *Photochem. Photobiol.* **1998**, *67*, 111.

JP806880S